RIPK3 acts as a lipid metabolism regulator contributing to inflammation and carcinogenesis in non-alcoholic fatty liver disease

Marta B. Afonso[1], Pedro M. Rodrigues[1], Miguel Mateus-Pinheiro[1], André L. Simão[1], Maria M. Gaspar[1], Amine Majdi[2,3], Enara Arretxe[4], Cristina Alonso[4], Álvaro Santos-Laso[5], Raúl Jimenez-Agüero[5], Emma Eizaguirre[5], Luis Bujanda[5], Maria Jesús Pareja[6], Jesús M. Banales[5], Vlad Ratziu[3,7,8], Jérémie Gautheron[2,3], Rui E. Castro[1], Cecília M. P. Rodrigues[1]

Author affiliations

[1]Research Institute for Medicines (iMed.ULisboa), Faculty of Pharmacy, Universidade de Lisboa, Lisbon, Portugal; [2]Sorbonne Université, Inserm, Centre de Recherche Saint-Antoine (CRSA), Paris, France; [3]Institute of Cardiometabolism and Nutrition (ICAN), Paris, France; [4]OWL Metabolomics, Bizkaia Technology Park, Derio, Spain; [5]Department of Liver and Gastrointestinal Diseases, Biodonostia Health Research Institute, Donostia University Hospital, University of the Basque Country (UPV/EHU), Ikerbasque, CIBERehd, San Sebastian, Spain; [6]Hospital de Valme, Sevilla, Spain; [7]Assistance Publique-Hôpitaux de Paris (AP-HP), Pitié-Salpêtrière Hospital, Department of Hepatology, Paris, France; [8]Sorbonne Université, Inserm, Centre de Recherche des Cordeliers (CRC), Paris, France

Correspondence to

Cecília M. P. Rodrigues, iMed.ULisboa, Faculty of Pharmacy, Universidade de Lisboa, Av. Prof. Gama Pinto, 1649-003 Lisbon, Portugal. E-mail: cmprodrigues@ff.ul.pt; phone: +351 21 7946490; fax: +351 21 7946491

Afonso MB, *et al. Gut* 2021;0:1–14. doi: 10.1136/gutjnl-2020-321767

Table of contents

Afonso MB, *et al. Gut* 2021;0:1–14. doi: 10.1136/gutjnl-2020-321767

Supplementary Materials and Methods

Patient cohorts

Non-alcoholic liver disease (NAFLD) liver specimens were obtained from two independent cohorts of patients. In cohort A, samples of frozen liver tissue were obtained from 71 individuals with risk factors for NAFLD (30 women and 41 men), who underwent diagnostic liver biopsy. Their age ranged from 29 to 74 years and the body mass index (BMI) from 26.0 to 38.7 kg/m^2. The study population was classified into three groups based on the histological scores of steatosis, lobular inflammation and fibrosis.[1] The first group included subjects with normal histology, *i.e.*, without steatosis (< 5%), inflammation or fibrosis (n=16). The second group included subjects with plain steatosis, also referred to as non-alcoholic fatty liver (NAFL), as defined by a steatosis score > 10% and both activity and fibrosis scores ≤ 2 (n=27). The third group included subjects with non-alcoholic steatohepatitis (NASH), as defined by a steatosis score > 10% and both activity and fibrosis scores > 2 (n=28). Liver tissue samples collected during percutaneous liver biopsy were immediately frozen in liquid nitrogen and stored at -80°C. All subjects gave written informed consent before taking part in this study. The procedure was approved by the Ethics Committee of the Pitié-Salpêtrière Hospital (Paris, France), and performed in accordance with the declaration of Helsinki.

In cohort B, liver tissue was prospectively and sequentially collected from 146 morbidly obese patients undergoing bariatric surgery. Biological data for each patient included haematological parameters, liver function tests and lipid profiles, which are summarized in **table S2**. One year after bariatric surgery, serum was also collected, and hepatic enzymes determined. Liver biopsies obtained at the same time as the bariatric surgery were fixed and processed for routine diagnosis and were blindly evaluated by an experienced pathologist. Liver histology was scored according to the NAFLD histology scoring system. Steatosis was graded from 0 to 3 based on the percentage of steatotic hepatocytes (0, <5%; 1, 5-33%; 2, 34–66%; 3, >66%). Lobular inflammation was graded from 0 to 3 based on the presence or absence of inflammatory cells under microscopic examination at x200 magnification (0, none; 1, <2 foci/field20x; 2, 2-4 foci; 3: >4 foci). Hepatocyte ballooning was graded from 0 to 2 by the presence of ballooned hepatocytes (0, none; 1, mild-poor; 2, moderate-high). Each liver specimen was assessed for the presence or absence of NASH by pattern recognition and for the NAFLD activity score (NAS), which is the sum of steatosis, inflammation and hepatocyte ballooning.[2] After Masson's Trichrome staining, portal and lobular fibrosis were semi-quantitatively graded on a scale of 0 to 4 (0, none; 1a, mild zone 3 perisinusoidal; 1b, moderate zone 3 perisinusoidal; 1c: only portal fibrosis; 2, zone 3 perisinusoidal and periportal; 3, bridging

fibrosis; 4, cirrhosis). In all patients, genomic DNA was isolated from EDTA anti-coagulated blood and the *PNPLA3* coding single nucleotide polymorphism (SNP) p.I148M (rs738409) as well as the *TM6SF2* p.E167K (rs58542926) and *MBOAT7* rs641738 variants were genotyped, as previously reported.[3] The study and sample collection were performed after informed consent and Institutional Review Board approval by the Donostia University Hospital (Sebastian, Spain), in accordance with the Declaration of Helsinki.

Animals and diets

Seven-to-eight-week-old male C57BL/6N wild-type mice (WT) or *Ripk3*-deficient mice (*Ripk3*$^{-/-}$) [4] from the same genetic background were fed either a choline-deficient L-amino acid-defined (CDAA) diet (Envigo, Madison, USA) or a control choline-sufficient L-amino acid-defined (CSAA) diet for 32 or 66 weeks. The phenotype remained completely stable over all experiments performed in different experimental groups. Six to seven animals were included in each experimental group. Mice were weighed monthly and food intake per cage measured weekly. At the indicated time-points, animals were fasted for 4 to 5 hours and sacrificed by CO_2 overdose. Blood was collected, the liver removed, and liver/body weight ratio determined. Part of epididymal white adipose tissue and the right lobe were collected, rinsed in normal saline and immediately flash-frozen in liquid nitrogen for protein and/or RNA extraction. The hepatic left lobe was fixed in paraformaldehyde (PFA; 4%, wt/vol) in phosphate buffered saline (PBS; Fisher Scientific, Inc., Waltham, MA, USA) for paraffin-embedded sectioning, while the median lobe and part of epididymal white adipose were included in optimal cutting temperature compound (Tissue-Tek OCT; Sakura Finetek Europe B.V., The Netherlands) for β-galactosidase activity assay and haematoxylin and eosin (H&E) staining, respectively. At 66 weeks, macroscopic discernible nodules were excised, rinsed in normal saline and immediately flash-frozen in liquid nitrogen for protein and RNA extraction or fixed in 4% PFA. HCC tissue samples were sectioned into two equal portions; one half was fixed in 4% PFA, and routine-processed for paraffin-embedding; the other half was frozen in liquid nitrogen. Liver paraffin-embedded sections (3-4 μm) were stained with H&E for routine histopathology by an experienced veterinary blinded pathologist, including evaluation of tumour subtype and growth pattern, steatosis, inflammatory infiltrates and hepatocyte ballooning, and were scored according to the NAS score as described for the cohort B NAFLD patients. Average of aggregates of ceroid-laden macrophages containing lipid-like pigment deposits were determined by 4 random microscope fields at x200 magnification. Fibrosis was graded from 0 to 4 (0, absent; 1, pericellular; 2, periportal and pericellular; 3, bridging fibrosis; 4, cirrhosis) following Masson's Trichrome

staining. Adipose tissue cryosections (4 μm) were stained with H&E for routine histopathology by an experienced veterinary blinded pathologist and inflammation was semi-quantitively graded from 0 to 5 (0, no changes; 1, minimal changes; 2, mild changes; 3 moderate changes; 4, marked changes; 5, severe, diffuse changes). To induce established liver tumorigenesis, thirteen to sixteen 2-week-old male pups were injected i.p. with 25 mg/kg diethylnitrosoamine (DEN, Sigma-Aldrich, Merck KGaA, Darmstadt, Germany) and were euthanized at the age of 42 weeks, followed by counting the number of tumours. All animal experiments were carried out with the permission of the local Animal Welfare Organ in accordance with the EU Directive (2010/63/EU), Portuguese laws (DL 113/2013, 2880/2015, 260/2016, and 1/2019) for the use and care of animals in research and all relevant legislations. The experimental protocol was approved by the competent national authority, *Direcção Geral de Alimentação e Veterinária*, Portugal. Animals received humane care in a temperature / humidity controlled environment with 12 hours light–dark cycles, complying with the Institute's guidelines, and as outlined in the "Guide for the Care and Use of Laboratory Animals" prepared by the National Academy of Sciences and published by the National Institutes of Health (NIH publication 86-23 revised 1985).

Serum analyses

Protein concentrations of human RIPK3 were determined in the serum from 34 subjects of the cohort A, including 8 with normal liver histology and 26 with NASH, by sandwich enzyme-linked immunosorbent assay (ELISA) according to the manufacturer's instructions (CSB-EL019737HU, CUSABIO Technology LLC, Houston, Texas, USA). In mice, after 4-5 hours fasting, euthanasia and blood collection, serum was isolated and hepatic transaminases, alkaline phosphatase, fasting glucose, triglycerides and free fatty acids determined using standard clinical chemistry techniques. In addition, ELISAs were used to determine fasting insulin (EZRMI-13K, Merck KGaA), fibroblast growth factor 21 (FGF-21; ab212160, Abcam Cambridge, United Kingdom), leptin (E06, Mediagnost®, Reutlingen, Germany) and adiponectin (E091-M, Mediagnost®) in mouse serum.

Glucose tolerance tests

Glucose tolerance tests were performed on 4-5 hours fasted mice after 31 weeks of CSAA or CDAA feeding (1 week before culling) through intraperitoneal injection of D-glucose at 2 g/kg of body weight. Fasting blood glucose was measured at baseline, 15, 30, 60, 90 and 120 minutes from a tail nick using a hand-held glucometer and test strips (Accu-Check® Sensor Comfort, Roche Diagnostics GmbH, Mannheim, Germany). WT

and *Ripk3*$^{-/-}$ mice fed with a standard diet were also subjected to a glucose tolerance test.

Hepatic triglycerides, free fatty acids and glycogen measurement

Liver triglycerides and free fatty acids contents were measured using the Triglyceride Quantification Kit (MAK266, Sigma-Aldrich, Merck) and Free Fatty Acid Quantitation Kit (MAK044, Sigma-Aldrich, Merck), respectively, following manufacturer's instructions. GloMax-Multi + Detection System (Promega Corp., Madison, WI, USA) was used to measure sample absorbance at 560 nm for triglycerides determination, and fluorescence intensity (λex=535/λem=590nm) for free fatty acids quantification. The amount of lipids was normalized by the liver mass. Hepatic glycogen was determined in murine livers using Glycogen Assay Kit II (ab169558, Abcam), according with supplier's instructions. Sample absorbance at 450 nm was measured using a Bio-Rad model 680 microplate reader (Bio-Rad Laboratories). The endogenous glucose background was determined for each sample and subtracted from sample reading. The amount of glycogen was normalized by the liver mass.

Quantitative RT-PCR

Total RNA was purified from frozen human liver tissue using TRIzol™ reagent (ThermoFisher, Waltham, MA, USA) and a RNeasy Mini kit (Qiagen, Courtaboeuf, France). The quantity and quality of RNA were determined spectroscopically using a Nanodrop (ThermoFisher). Total RNA (2 μg) was used to synthesize cDNA using the M-MLV reverse transcriptase kit (ThermoFisher) according to the manufacturer's protocol. The cDNA samples were used for quantitative real-time RT-PCR (qPCR) in a total volume of 10 μl using SYBR Green Reagent (Roche Diagnostics, Meylan, France) and specific primers listed in **table S3**, on a LightCycler 96 Roche Instrument. All RT-qPCRs were performed in duplicate. All values were normalized for the level of glyceraldehyde-3-phosphate dehydrogenase (*GAPDH*).

RNA was also extracted from animal liver and *epididymal* white *adipose* samples using the TRIzol™ reagent and total RNA was quantified in a Qubit™ 2.0 fluorometer (Thermo Fisher Scientific). Total RNA (1.5 μg) was converted into cDNA using NZY First-Strand cDNA Synthesis Kit (NZYTech, Lisbon, Portugal), according to the manufacturer's instructions. qPCR was performed in 5 μL duplicate reactions on a 384-well QuantStudio 7 Flex Real-Time PCR System (Applied Biosystems, Thermo Fisher Scientific), using the 2x SensiFAST SYBR Hi-ROX kit (Bioline*, Meridian Bioscience,* Inc., Cincinnati, OH, USA), following manufacturer's protocol. Primer sequences are listed in **table S3**. The relative amounts of each gene were calculated based on the standard curve normalized

to the level of *Hrpt* and expressed as fold change from CSAA WT mice at each respective time-point, except for the microarray validation where β-actin was used as reference gene and results expressed as fold change from non-tumoral tissue of CDAA WT mice.

Mouse liver cancer genes array

Differential gene expression in non-tumoral tissue (NT) from CDAA-fed WT mice *versus* NT from CDAA-fed *Ripk3*$^{-/-}$ mice or tissue enriched in preneoplastic nodules from CDAA-fed WT or *Ripk3*$^{-/-}$ mice was evaluated using a RT² Profiler™ Mouse Liver Cancer PCR Array (PAMM-133Z, Qiagen, MD, USA) according to the manufacturer's instructions. RNA was quantified in a Qubit™ 2.0 fluorometer (Invitrogen, Thermo Fisher Scientific), whereas its quality and integrity was evaluated in a Nanodrop™ ND-1000 Spectrophotometer (NanoDrop Technologies, Thermo Fisher Scientific, Waltham, MA USA) and on denaturation agarose gel, respectively. Equal amounts of total RNA from animals on each experimental group were pooled and 0.5 µg of total of DNase I-treated RNA (Roche) was used to synthesize single stranded cDNA, using the RT^2 First Strand Kit (Qiagen), following the manufacturer's protocol. qRT-PCR was run on a 96-well Applied Biosystems 7300 system (Thermo Fisher Scientific), using the RT^2 SYBR Green ROX qPCR master mix (Qiagen). Quality controls for PCR array reproducibility, reverse transcription efficiency and genomic DNA contamination were included. β-actin was used as endogenous control. Data analysis was performed using the GeneGlobe online platform (https://www.qiagen.com/geneglobe/). Relative gene expression over NT CDAA WT mice was determined as per the comparative cycle threshold ($2^{-\Delta\Delta Ct}$) method ($\Delta Ct = Ct^{target} - Ct^{\beta\text{-actin}}$; $\Delta\Delta Ct = \Delta Ct^{tested\ condition} - \Delta Ct^{NT\ CDAA\ WT}$). Only mRNAs whose expression was dysregulated by a $\log_2$-fold change ≥ 0.58 and ≤ -0.42, compared to NT CDAA WT, were considered differentially expressed transcripts. Results for each detectable gene are shown in **table S4.**

Gene ontology (GO) biological process and Kyoto Encyclopedia of Genes and Genomes (KEGG) pathway enrichment were performed for the functional analysis of differentially expressed genes using the Cytoscape software (version 3.7.2, Cytoscape Consortium, http://www.cytoscape.org/).[5] Discovery Rate (FDR) adjusted *p* value < 0.05 results were considered as statistically significant. Census of cancer genes database (COSMIC, https://cancer.sanger.ac.uk/cosmic) was used to identify oncogenes.

Protein extraction and immunoblotting

Steady-state levels of selected proteins were determined by immunoblot analysis. For isolation of total protein extracts, frozen mouse (~25 mg) or human (~10 mg) liver tissue

was homogenized using a motor-driven grinder on ice-cold lysis buffer (10 mM Tris-HCl, pH 7.6, 5 mM $MgCl_2$, 1.5 mM potassium acetate, 1% Nonidet P-40, 2 mM dithiothreitol) and 1x Halt Protease and Phosphatase Inhibitor Cocktail (Pierce, Thermo Fisher Scientific). The lysate was centrifuged at 10,000 *g* for 10 min at 4°C and the supernatant recovered and stored at -80ºC. Briefly, 40 µg of total protein extracts were separated on an 8 or 12% sodium dodecyl sulfate-polyacrylamide gel electrophoresis (SDS-PAGE). Following electrophoretic transfer onto nitrocellulose membranes and blocking with 5% milk solution, blots were incubated overnight at 4°C with primary rabbit polyclonal antibodies against α-fetoprotein (AFP; 1:200, sc-130302; Santa Cruz Biotechnology Inc., Dallas, TX, USA), aldehyde dehydrogenases (ALDH 1/2; 1:200, #sc-50385, Santa Cruz Biotechnology Inc.), β-catenin (1:500, 13-8400, Thermo Fisher Scientific Inc.), γ-H2AX (1:2500, #ab2893, Abcam); Nanog (1:1000, 8822, Cell Signaling Technology Inc., Danvers, MA, USA); cyclin D1 (1:200, sc-20044, Santa Cruz Biotechnology Inc.), p-MLKL (1:1000, ab196436, Abcam), mixed lineage kinase domain-like protein (MLKL; 1:500, SAB1302339, Sigma-Aldrich, Merck), PPARγ (1:1000, ab41928, Abcam,), p21 (1:200, sc-397, Santa Cruz Biotechnology Inc.), p-p38 (1:1000, 9211, Cell Signaling Technology,), p38 (1:200, sc-7972, Santa Cruz Biotechnology Inc.), p53 (1:1000, #2524, Cell Signaling Technology), receptor-interacting serine/threonine-protein kinase 3 (RIPK3; for mouse samples: 1:1000, AHP1797, AbD Serotec, Bio-Rad Laboratories, Hercules, CA, USA; for human samples; 1:1000, ab56164, Abcam) and Vimentin (1:200, sc-32322, Santa Cruz Biotechnology Inc.). Following, incubation with a secondary antibody conjugated with horseradish peroxidase (Bio-Rad Laboratories) diluted 1:5000 in blocking solution for 1 - 3 hours at room temperature, membranes were processed for protein detection by chemiluminescence using Super Signal substrate (Pierce, Thermo Fisher Scientific Inc.), on a ChemiDoc XRS+ imaging system (Bio-Rad). β-actin (1:40,000; A5541; Sigma-Aldrich, Merck) was used as loading control. The relative intensities of protein bands were analyzed using the Image Lab densitometric analysis program (version 5.1; Bio-Rad Laboratories, Hercules, CA, USA).

Immunofluorescence, immunohistochemistry and image analysis

Paraffin-embedded human and mouse liver sections were deparaffined in xylene, rehydrated in graded ethanol and boiled three times in 10 mM citrate, pH 6.0. For immunofluorescence, sections were then incubated in 10% normal goat serum (Jackson ImmunoResearch Laboratories, Inc., West Grove, PA, USA), 1% fetal bovine serum (FBS; Thermo Fisher Scientific, Inc.) and 0.3% Triton X-100 in 0.1% Tween-PBS for 1h to block non-specific protein-protein interactions, followed by an incubation with a primary antibody reactive to human RIPK3 (1:75, ab56164, Abcam) overnight at 4°C.

After three 0.1% Tween-PBS washes, the primary antibody was developed by incubating with a 1:200 secondary Alexa Fluor 568-conjugated donkey anti-rabbit antibody (Thermo Fisher Scientific) for 2 hours at room temperature. Nuclei were stained with Hoechst 33258 at 50 µg/mL in PBS for 10 minutes at room temperature. After extensive rising, samples were mounted using Mowiol 4-88 (Sigma-Aldrich, Merck). Detection of RIPK3 was visualized using an AxioScope.A1 microscope (Carl Zeiss Microscopy GmbH, Jena, Germany). Images were acquired using an AxioCam HRm camera with the with the Zen Lite 2012 (blue edition) for image acquisition (version 1.1.2.0, Carl Zeiss Microscopy GmbH). Eight images *per* sample were obtained for each sample and used for the semiquantitative analysis of mean fluorescence intensities of RIPK3. Images were converted into an 8-bit format using the FIJI software (ImageJ, National Institute of Health, Bethesda, USA), and the background was subtracted. A threshold optical density was set and kept constant for all images analyzed. RIPK3 fluorescence intensity was normalized with the area of liver tissue per microscopic field.

For Ki67 immunohistochemistry, after deparaffinization/rehydration and antigen retrieval, endogenous peroxidase was inactivated by incubating sections in 3% hydrogen peroxide for 10 minutes at room temperature. Subsequently, sections were incubated for 1 hour in blocking buffer at room temperature. Primary antibody reactive to Ki67 (1:100; ab16667, Abcam) was incubated overnight at 4ºC. Detection of the primary antibody was performed using the HiDef Detection HRP Polymer System (Cell Marque, Rocklin, CA, USA), according to the manufacturer's instructions. Sections were developed using SIGMAFAST 3,3′-diaminobenzidine (DAB) tablets (Sigma-Aldrich, Merck) and counterstained with Gill's haematoxylin for 3 minutes. Finally, liver sections were differentiated with 37.5% HCl and immediately rinsed with water, dehydrated and mounted with a glass coverslip using Entellan mounting media (Merck Millipore). The specimens were examined using an Axio Scope bright-field microscope (Zeiss Axioskop; Carl Zeiss GmbH, Jena, Germany). Images were acquired using a DFC490 camera (Leica Microsystems AG, Heersbrugg, Switzerland) with the Zen Lite 2012 (blue edition) for image acquisition. The frequency of Ki67-positive cells was measured in 8 microscopic fields displaying similar cell density per sample and results expressed as the percentage of Ki67-positive cells per field.

F4/80 immunohistochemistry was conducted by deparaffinizing and rehydrating sections, followed by inactivation of endogenous peroxidase as described above. Thereafter, sections were treated with 20 µg/mL Proteinase K (Invitrogen, Thermo Fisher Scientific) at 37ºC for 20 min and permeabilized with 0.25% Triton X for 10 minutes at room temperature. Endogenous avidin, biotin and biotin-binding proteins in tissues were blocked using the avidin-biotin blocking kit (Vector laboratories, Burlingame, CA, USA).

Tissue sections were subsequently incubated with blocking buffer for 30 minutes at room temperature, primary antibody reactive to F4/80 (1:100; ab6640, Abcam) overnight at 4ºC and biotinylated anti-rat antibody (1:200, STAR131B, Bio-Rad Laboratories) for 50 minutes at room temperature. Sections were developed using Vectastain® Elite® ABC Reagent (Vector laboratories) followed by incubation Vector DAB Substrate (Vector laboratories). Finally, liver sections were counterstained with Gill's for 3 minutes. Finally, liver sections counterstained with haematoxylin, differentiated with HCl, dehydrated and mounted with a glass coverslip using Entellan. Brightfield images of liver sections were acquired using EVOS FL Auto 2 Cell Imaging System (Invitrogen, Thermo Fisher Scientific). F4/80-positive stained areas were determined in 8 microscopic fields *per* sample using the FIJI software and normalized with the area of liver tissue per microscopic field. Negative controls with the omission of the primary antibody were used for validation for all staining procedures.

β-galactosidase activity

β-galactosidase activity at pH 6, a known characteristic of senescent cell, was assessed in mouse liver cryosections using the Senescence β-galactosidase kit (9860S; Cell Signaling Technology), according to the manufacturer's instructions. Briefly, cryosections (4 μm) were fixed with 1X fixative solution provided by the commercial kit for 15 minutes at room temperature, washed in PBS and immersed overnight in β-galactosidase staining solution at 37°C in a dry incubator (no CO_2). Thereafter, slides were briefly rinsed in PBS and mounted with a glass coverslip using 70% glycerol. The specimens were examined using EVOS FL Auto 2 Cell Imaging System. The frequency of β-galactosidase positive cells was measured in 10 microscopic fields and normalized with the area of liver tissue per microscopic field. Negative controls with the omission of β-galactosidase staining solution were used for validation for β-galactosidase activity assay.

Analysis of liver hydroxyproline content, total reactive oxygen species and caspase-3/-7 activity

Total collagen content in the mouse liver was estimated by measuring the collagen-specific amino acid hydroxyproline using a commercial colorimetric kit (Hydroxyproline Assay Kit; Sigma-Aldrich, Merck), as previously described.[6] Total reactive oxygen species (ROS) levels and caspase-3/-7 activity were analysed in whole liver lysates through the use of 2′,7′-dichlorodihydrofluorescein diacetate (H_2DCFDA) (Sigma-Aldrich, Merck) and Caspase-Glo 3/7 Assay (Promega Corp.), respectively, as mentioned before.[7]

Lipidomic analysis

Two separate liquid chromatography (LC)-time of flight (ToF)-mass spectrometry (MS)-based platforms that analysed methanol (Platform 1) and methanol/chloroform (Platform 2) extracts for lipid analyses were used for the lipidomics analysis.[8] Identified metabolites in the methanol extract platform included fatty acids, acyl carnitines, bile acids, lysoglycerophospholipids, free sphingoid bases, N-acyl ethanolamines and oxidized fatty acids. The chloroform/methanol extract platform provided coverage over glycerolipids, cholesterol esters, sphingolipids and glycerophospholipids.

Briefly, proteins were precipitated by adding H_2O (15:1, v/w), methanol containing the internal standards used for platform 1 (50:1, v/w), chloroform:methanol (2:1) containing internal standards used for platform 2 (4:1, v/w) and chloroform (40:1, v/w) to the liver tissue (15 mg). The homogenization of the resulting mixture was performed using a Precellys 24 homogenizer (Bertin Technologies, Montigny-le-Bretonneux, France) at 6500 rpm for 45 seconds x 1 round. Homogenized samples were incubated at -20 °C for 1 hour and after vortexing, 500 µL were collected for each platform. For Platform 1, supernatants were centrifugated, dried under vacuum and reconstituted in methanol. For Platform 2, the supernatants were mixed with ammonium hydroxide in H_2O (pH 9) and incubated for 1 hour at -20 °C. After centrifugation, the organic phase was collected and dried under vacuum. Dried extracts were reconstituted in acetonitrile / isopropanol (1:1) for LC-MS analysis.

Data were pre-processed using the TargetLynx application manager for MassLynx 4.1 software (Waters Corp., Milford, USA). Metabolites were identified prior to the analysis. A total of 392 metabolic features were detected in the analysed liver samples and included in the subsequent univariate and multivariate data analysis. Lipid nomenclature and classification follows the LIPID MAPS convention, www.lipidmaps.org. Intra- and inter-batch normalization was performed by inclusion of multiple internal standards and pool calibration response correction, as previously described.[9] Volcano plot analysis was performed as an easy-to-understand graph that summarizes fold-change and significance. It is a scatterplot of the negative $\log_{10}$-transformed *p* values from the *t* test against the $\log_2$ fold-change. All calculations were performed using the statistical software package R v.3.4.0 (R Development Core Team, 2017). Multivariate principal component analysis (PCA) was performed with the software SIMCA 14.1 (Umetrics, Malmo, Sweden).

Cell culture and treatments

Primary mouse hepatocytes were isolated from male WT and *Ripk3* $^{-/-}$ mice as previously described.[10 11] After isolation, hepatocytes were resuspended in Complete William's E medium (Sigma-Aldrich, Merck) and plated on Primaria™ tissue culture dishes (BD Biosciences, San Jose, CA, USA) at 5×10^4 cells/cm^2. Cells were maintained at 37°C in a humidified atmosphere of 5% CO_2 for 4 h, to allow attachment. Then, primary mouse hepatocytes were transfected with 30 µM of a short interference RNA (siRNA) nucleotide against *Pparγ* (siPPARγ) designed to knock down *Pparγ* gene expression in mouse (Silencer® Select Pparag mouse assay, s72013, Thermo Fisher Scientific), or a siRNA control (siControl; Silencer™ Select Negative Control No. 1, Thermo Fisher Scientific), using Lipofectamine 3000™ (Invitrogen, Thermo Fisher Scientific Inc.), according to manufacturer's instructions. At 16 h post-transfection, cells were treated with 400 µM palmitic acid (PA, Sigma-Aldrich, Merck) or vehicle control (dimethyl sulfoxide, DMSO; Sigma-Aldrich, Merck) for 24 h. Cells were then harvested for Nile Red staining and total RNA isolation. Nile Red Staining allows the fluorometric measurement of intracellular lipid droplets. For Nile Red staining, cells plated on a 96-well plate were incubated with 5 µg/mL Nile red (Sigma-Aldrich, Merck) diluted in cell culture medium (100 µL per well) at 37ºC in a CO_2 incubator for 90 minutes. Cells were then washed with PBS to remove the excess of dye and fluorescence intensity (λex=552/λem=636nm) was measured using Varioskan™ LUX multimode microplate reader (Thermofisher). Fluorescence values were corrected with total protein content.

The human hepatic stellate cell line LX-2 (Merck), was cultured in Dulbecco's modified Eagle's medium (DMEM) supplemented with 2% FBS, penicillin (100 units/ml), streptomycin (100 µg/ml) and 2 mM L-glutamine (Thermo Fisher Scientific). LX-2 cells were seeded at a density of $2x10^5$ cells per well in 6-well plates for 24 hours. Cells were co-transfected with siRNA against human *PPARγ* (Silencer™ Select Pre-Designed siRNA human PPARG, s10886, Thermo Fisher Scientific) and *RIPK3* (Silencer™ Select Pre-Designed siRNA human RIPK3, s21742, Thermo Fisher Scientific) or siControl in 4 different combinations: 1) siControl; 2) siControl + siPPARγ; 3) siRIPK3 + siControl; 4) siRIPK3 + siPPARγ). At 24 hours post-transfection, cells were treated with 2 ng/mL TGFβ1 Recombinant Human Protein (Thermo Fisher Scientific). After 24 hours, cells were harvested for total protein and RNA isolation. Experiments were performed on 3 independent cell preparations, used between passages 2 and 7.

Pparγ promoter luciferase assay

For the promoter reporter luciferase assay, we used Gluc-ON promoter reporter clone of *Pparγ* in vector pEZX-PG04 expressing the secreted Gaussian luciferase under the control of the specific promoter and expressing constitutively the secreted alkaline phosphatase under CMV (MPRM38531-PG04, Genecopoeia, Inc., Rockville, MD). Briefly, primary hepatocytes cells were plated on a 96-well plate and transfected with 100 ng of plasmid per well using Lipofectamine 3000™ for 16 hours and treated with 400 µM palmitic acid (Sigma-Aldrich, Merck) or vehicle control for 24 hours. The promotor reporter activity was measured using the Secrete-Pair™ Dual Luminescence Assay Kit (Genecopoeia), according to the manufacturer's instructions. FB12 Tube Luminometer (Berthold Detection Systems GmbH, Pforzheim, Germany) was used to measure luminescence intensity. Secreted alkaline phosphatase signal was used as an internal standard control.

Additional References used in Supplementary Materials and Methods

1. Bedossa P, Consortium FP. Utility and appropriateness of the fatty liver inhibition of progression (FLIP) algorithm and steatosis, activity, and fibrosis (SAF) score in the evaluation of biopsies of nonalcoholic fatty liver disease. *Hepatology* 2014;**60**:565-75.

2. Kleiner DE, Brunt EM, Van Natta M, et al. Design and validation of a histological scoring system for nonalcoholic fatty liver disease. *Hepatology* 2005;**41**:1313-21.

3. Krawczyk M, Jimenez-Aguero R, Alustiza JM, et al. PNPLA3 p.I148M variant is associated with greater reduction of liver fat content after bariatric surgery. *Surg Obes Rel Dis* 2016;**12**:1838-46.

4. Newton K, Sun X, Dixit VM. Kinase RIP3 is dispensable for normal NF-kappa Bs, signaling by the B-cell and T-cell receptors, tumor necrosis factor receptor 1, and Toll-like receptors 2 and 4. *Mol Cell Biol* 2004;**24**:1464-9.

5. Shannon P, Markiel A, Ozier O, et al. Cytoscape: a software environment for integrated models of biomolecular interaction networks. *Genome Res* 2003;**13**:2498-504.

6. Afonso MB, Rodrigues PM, Simao AL, et al. miRNA-21 ablation protects against liver injury and necroptosis in cholestasis. *Cell Death Differ* 2018;**25**:857-72.

7. Afonso MB, Rodrigues PM, Simao AL, et al. Activation of necroptosis in human and experimental cholestasis. *Cell Death Dis* 2016;**7**:e2390.

8. Barr J, Caballeria J, Martinez-Arranz I, et al. Obesity-dependent metabolic signatures associated with nonalcoholic fatty liver disease progression. *J Proteome Res* 2012;**11**:2521-32.

9. Martinez-Arranz I, Mayo R, Perez-Cormenzana M, et al. Enhancing metabolomics research through data mining. *J Proteomics* 2015;**127**:275-88.

10. Afonso MB, Rodrigues PM, Carvalho T, et al. Necroptosis is a key pathogenic event in human and experimental murine models of non-alcoholic steatohepatitis. *Clinical Sci* 2015;**129**:721-39.

11. Castro RE, Ferreira DM, Zhang X, et al. Identification of microRNAs during rat liver regeneration after partial hepatectomy and modulation by ursodeoxycholic acid. *Am J Physiol Gastrointest Liver Physiol* 2010;**299**:G887-97.

Table S1 Correlation of RIPK3 levels in human NAFLD cohorts with clinical and biochemical parameters

		p	**Spearman/ Pearson r**
Cohort A	*CD38* mRNA levels	<0.0001	0.483
	CD68 mRNA levels	0.0001	0.429
	ARG1 mRNA levels	ns	0.045
	RIPK1 mRNA levels	0.0001	0.425
	CASPASE-3 mRNA levels	0.097	0.192
	CASPASE-1 mRNA levels	<0.0001	0.584
	TGFβ1 mRNA levels	<0.0001	0.534
Cohort B	Ferritin (ng/mL)	0.029	0.241
	Platelets (K/μL)	0.025	-0.202
	Glucose (mg/dL)	ns	-0.032
	Glucose post-bariatric surgery (mg/dL)	ns	-0.011
	Triglycerides (mg/dL)	ns	0.090
	Total Cholesterol (mg/dL)	ns	0.062
	HDL Cholesterol (mg/dL)	ns	-0.011
	LDL Cholesterol (mg/dL)	ns	0.047
	Alkaline Phosphatase (U/L)	ns	0.138
	Creatinine (mg/dL)	0.070	0.161
	Hemoglobin (g/dL)	ns	0.062
	Albumin (g/dL)	ns	0.101
	Total bilirrubin (mg/dL)	ns	0.124
	Age (years)	0.057	0.160
	Height (cm)	ns	0.147
	Weight (kg)	ns	0.083
	BMI (kg/m^2)	ns	-0.035

ARG1**,** arginase-1; BMI, body mass index; CD, cluster of differentiation; HDL, high-density lipoprotein; LDL, low-density lipoprotein; RIPK1, receptor-interacting serine/threonine-protein kinase 1; TGFβ1, transforming growth factor-β. Association between two variables was assessed by Pearson or Spearman correlation coefficient for normally and nonnormally distributed data, respectively. ns, non-significant.

Table S2 Demographic, clinical and laboratory data of NAFLD patients from Cohort B

Cohort B	**NAFLD (n = 146)**
Age (years)	48 ± 1.1
Gender (M/F)	53/93
BMI ((kg/m^2)	45 ± 0.6
ALT (U/L)	29.6 ± 1.5
AST (U/L)	23.1 ± 0.8
GGT (U/L)	38.3 ± 3.3
ALP(U/L)	75.2 ± 2.5
Cholesterol (mg/dL)	202.7 ± 3.9
HDL Cholesterol (mg/dL)	49.5 ± 1.1
LDL Cholesterol (mg/dL)	122.5 ± 3.1
Triglycerides (mg/dL)	145.8 ± 7.8
Glucose (mg/dL)	111.3 ± 2.2
Total bilirrubin (mg/dL)	0.48 ± 0.02
Creatinine (mg/dL)	0.74 ± 0.02
Hemoglobin (g/dL)	13.7 ± 0.1
Albumin (g/dL)	4.12 ± 0.04
Ferritin (ng/mL)	140.6 ± 19.7
Platelets (K/µL)	257464 ± 5073

Data are presented as mean ± SEM.

Table S3 Primer sequences for quantitative RT-PCR

	Gene	Forward primer(5' → 3')	Reverse primer (5' → 3')
Human	*ARG1*	CCCTGGGGAACACTACATTTTG	GCCAATTCCTAGTCTGTCCACTT
	CASP1	TTTCCGCAAGGTTCGATTTTCA	GGCATCTGCGCTCTACCATC
	CASP3	AGAGGGGATCGTTGTAGAAGTC	ACAGTCCAGTTCTGTACCACG
	CD38	AGACTGCCAAAGTGTATGGGA	GCAAGGTACGGTCTGAGTTCC
	CD68	TGGGGCAGAGCTTCAGTTG	TGGGGCAGGAGAAACTTTGC
	COL1A1	GTGCGATGACGTGATCTGTGA	CGGTGGTTTCTTGGTCGGT
	GAPDH	AGAAGGCTGGGGCTCATTTG	AGGGGCCATCCACAGTCTTC
	IL1B	TTCGACACATGGGATAACGAGG	TTTTTGCTGTGAGTCCCGGAG
	MLKL	AGGAGGCTAATGGGGAGATAGA	TGGCTTGCTGTTAGAAACCTG
	NLRP3	GATCTTCGCTGCGATCAACAG	CGTGCATTATCTGAACCCCAC
	PPARγ	CTCGAGGACACCGGAGAGG	CACGGAGCTGATCCCAAAGT
	RIPK1	GGGAAGGTGTCTCTGTGTTTC	CCTCGTTGTGCTCAATGCAG
	RIPK3	AATTCGTGCTGCGCCTAGAAG	TCGTGCAGGTAAAACATCCCA
	TGFB1	CAATTCCTGGCGATACCTCAG	GCACAACTCCGGTGACATCAA
	TNFA	GAGGCCAAGCCCTGGTATG	CGGGCCGATTGATCTCAGC
Mouse	*Acc*	GGACACCAGTTTTGCATTGA	AGTTTGGGAGGACATCGAAA
	Akt1	TAGGCCCAGTCGCCCG	TATTCCCCTCGTTTGTGCAGC
	α-Sma	GCTACGAACTGCCTGACGG	GCTGTTATAGGTGGTTTCGTGGA
	Actb	GTGGGCCGCTCTAGCACCAA	CTCTTTGATGTCACGCAGGATTTC
	Cdkn1a	CAGACATTCAGAGCCACAGGC	CAAAGTTCCACCGTTCTCGG
	Cox-2	CAGCCAGGCAGCAAATCCTT	AGTCCGGGTACAGTCACACT
	F4/80	GCATCATGGCATACCTGTTC	GAGCTAAGGTCAGTCTTCCT
	Fasn	AAGTTGCCCGAGTCAGAGAAC C	ATCCATAGAGCCCAGCCTTCCATC
	Hrpt	GGTGAAAAGGACCTCTCGAAGTG	ATAGTCAAGGGCATATCCAACAACA
	Mcad	GGGGGAAAGGCCAACTGGTAT	ATCGCTGGCCCATGTTTAGT
	Mip-2	GCTACGAACTGCCTGACGG	GCTGTTATAGGTGGTTTCGTGGA
	Nlrp3	AGAGCCTACAGTTGGGTGAAATG	CCACGCCTACCAGGAAATCTC
	p16	TGGTCACTGTGAGGATTCAGC	TTGCCCATCATCATCACCTGG
	Pparγ	GATGCACTGCCTATGAGCAC	TCTTCCATCACGGAGAGGTC
	Rac	GCCTGCTCATCAGTTACACG	ACATGTGTCTCCAACTGTCTGC
	Rhoa	GGTCCTCCGTCGGTTCTCTC	GATGCAAGGCTCAAGGCGAG
	Tlr4	TCCCTGCATAGAGGTAGTTCCTA	CTTCAAGGGGTTGAAGCTCAG
	Tnf-α	AGGCACTCCCCCAAAAGATG	TGAGGGTCTGGGCCATAGAA
	Ucp1	AAGGTCAGAATGCAAGCCCA	ATTAGGGGTCGTCCCTTTCCA
	Vlcad	CAGCGACTTTATGCCAGGGA	TGGCAGGGTCATTCACTTCC

Table S4 Analysis of mouse liver cancer-related genes using the RT² Profiler™ PCR Array

Gene	NT CDAA *Ripk3*$^{-/-}$ *vs.* NT CDAA WT (log_2 fold change)	Nodules WT *vs.* NT CDAA WT (log_2 fold change)	Nodules *Ripk3*$^{-/-}$ *vs.* NT CDAA WT (log_2 fold change)
Adam17	-0.06	0.28	-0.15
Akt1	0.18	0.71	-0.15
Angpt2	0.11	0.11	0.28
Bax	0.07	-0.17	0.21
Bcl2	0.24	-0.17	0.38
Bcl2l1	0.31	0.23	-0.04
Bid	-0.15	0.39	-0.40
Birc2	0.48	0.55	0.33
Birc5	0.52	1.02	0.50
Casp8	0.32	0.48	0.25
Ccl5	-0.60	-0.60	-0.27
Ccnd1	-0.09	0.70	-0.30
Ccnd2	0.19	0.77	0.42
Cdh1	-0.09	-0.15	0.03
Cdh13	0.21	0.46	-0.06
Cdkn1a	0.99	0.04	1.13
Cdkn1b	0.11	0.53	0.06
Cdkn2a	-0.47	-2.00	-0.86
Cflar	-0.15	0.48	-0.18
Ctnnb1	-0.07	0.58	-0.22
Cxcr4	-0.15	0.81	0.70
Dab2ip	0.03	-0.32	0.18
Dlc1	-0.41	0.44	-0.06
E2f1	0.24	-0.60	-0.20
Egf	0.11	-0.29	-1.40
Egfr	-1.09	-0.22	-1.56
Ep300	-0.25	0.10	-0.01
Fadd	-0.42	-0.32	-0.58
Fas	0.03	0.57	-0.17
Fhit	0.37	0.76	0.30
Flt1	0.66	0.24	0.85
Fzd7	-0.14	0.11	-0.51
Gadd45b	0.03	-0.42	0.03
Gstp1	-0.60	-0.84	-0.62
Hgf	0.29	0.57	0.18
Hhip	-0.64	0.96	-1.15
Hras	0.19	0.14	0.07
Igf2	0.68	0.49	1.72
Igfbp1	1.67	1.06	2.31

Igfbp3	1.04	0.90	0.90
Irs1	-1.15	-0.38	-1.56
Itgb1	0.30	0.64	0.07
Kdr	-0.36	0.08	-0.49
Lef1	0.39	0.31	1.24
Mcl1	0.24	0.68	0.14
Met	-0.12	0.10	-0.30
Msh2	-0.38	-0.56	-0.18
Msh3	0.14	0.52	-0.06
Mtdh	0.24	0.79	0.32
Myc	-0.03	-0.74	0.89
Nfkb1	-0.12	-0.06	-0.15
Nras	-0.06	0.56	0.03
Opcml	1.95	1.26	1.93
Pdgfra	0.33	0.30	0.90
Pin1	0.23	0.23	-0.25
Pten	0.08	0.61	0.00
Ptgs2	0.12	3.48	2.07
Ptk2	0.03	0.23	-0.20
Pycard	0.00	0.76	0.00
Rac1	0.30	0.93	0.24
Rassf1	0.04	0.04	0.12
Rb1	-0.03	0.46	-0.04
Reln	-0.27	-0.12	-0.12
Rhoa	0.07	0.60	0.03
Runx3	-0.10	0.18	0.86
Sfrp2	-1.18	-0.92	-1.06
Smad4	-0.30	0.00	-0.34
Smad7	-0.58	-1.15	-0.69
Socs1	-0.49	0.52	-1.12
Socs3	-0.40	-0.20	-0.17
Stat3	-0.40	-0.67	-0.67
Tcf4	0.00	0.54	0.10
Tert	-0.10	-0.25	0.08
Tgfa	-0.07	0.12	0.26
Tgfb1	-0.32	-0.17	-0.30
Tgfbr2	-0.27	-0.34	-0.15
Tlr4	0.06	0.52	0.03
Tnfrsf10b	-0.22	0.41	-0.22
Tnfsf10	-0.36	0.91	-0.25
Trp53	-0.34	-0.84	-0.41
Vegfa	0.37	0.60	0.06
Wt1	0.46	0.11	0.23
Xiap	-0.22	0.79	-0.23
Yap1	-0.20	0.15	-0.20

Figure S1

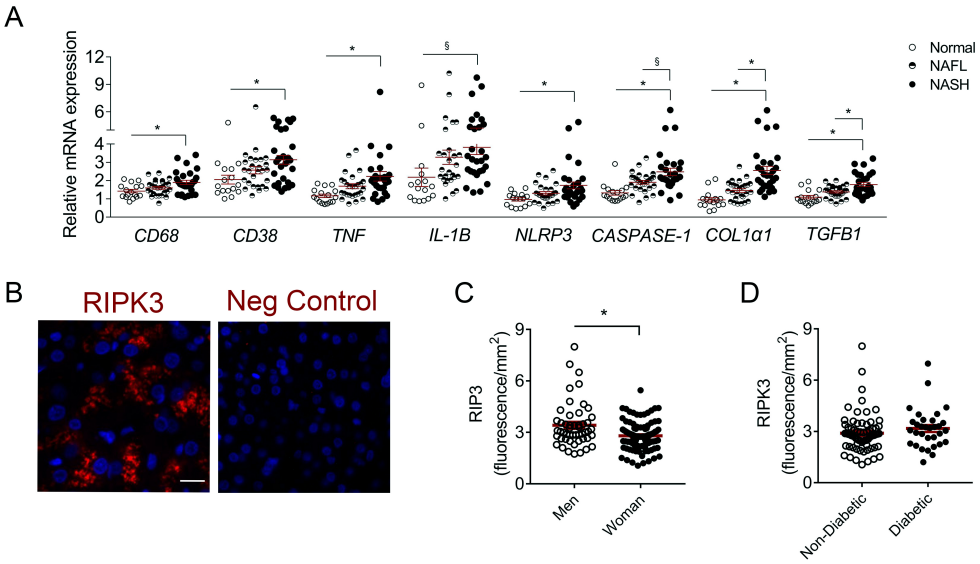

Figure S1 Inflammatory and fibrosis markers mRNA levels in patients. (A) qRT-PCR analysis of *CD68, CD38, TNF, IL-1β, NLKLPR, CASPASE-1, COL1α1, TGF-β* in the liver of cohort A NAFLD patients (n = 71). (B) Representative higher magnification of RIPK3 immunofluorescence (red) in liver sections from cohort B NAFLD patients. Scale bar = 100 μm (*left*). Representative rabbit IgG negative controls are shown (*right*). Histogram show the quantification of RIPK3 levels assessed by immunofluorescence according to gender (C) and the presence of Diabetes Mellitus (D) of NAFLD patients from cohort B (n = 146). Each individual is represented by one dot and results are expressed as mean ± SEM arbitrary units or fold change. $^{\S}p < 0.05$ and $^{*}p < 0.01$.

Figure S2

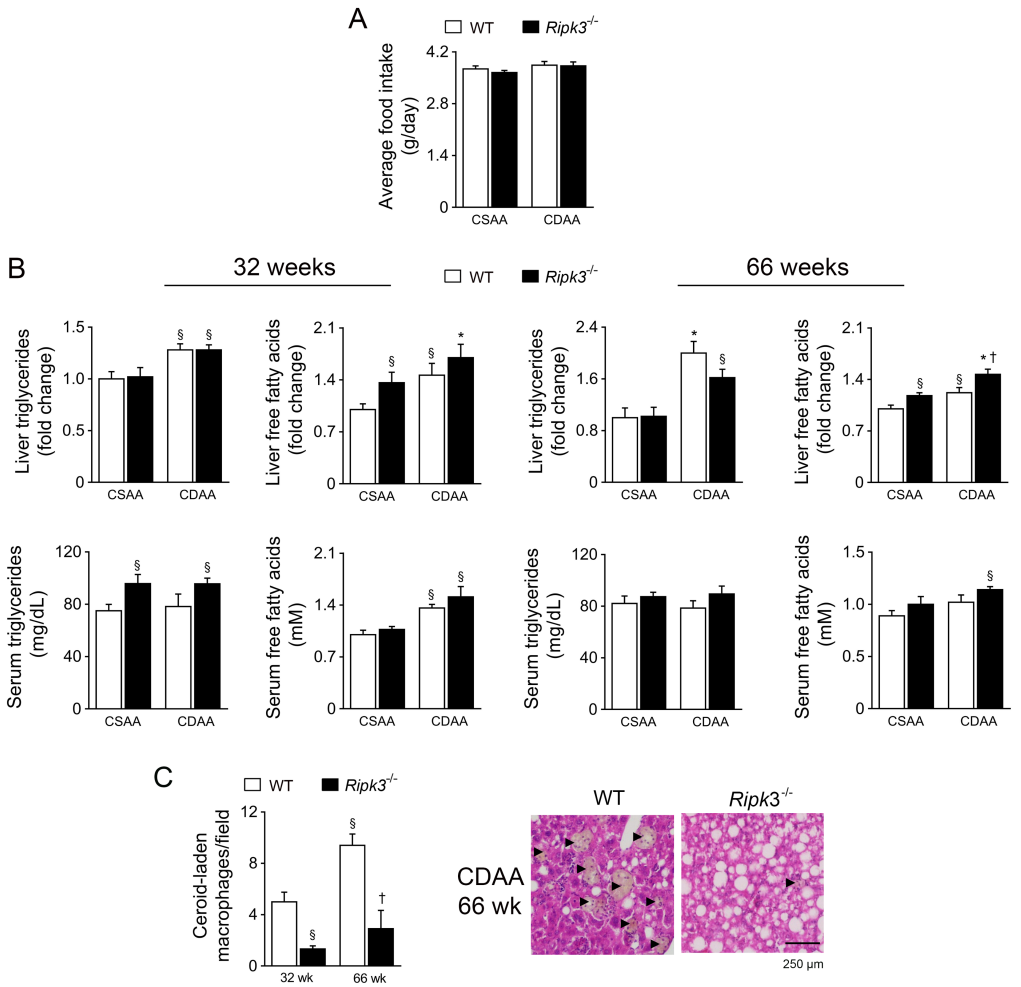

Figure S2 Daily food intake and lipid content of liver and serum from CDAA-fed mice. (A) Average daily food intake of C57BL/6 WT or *Ripk3*$^{-/-}$ mice fed a CDDA or an isocaloric control CSAA for 32 or 66 weeks. (B) Liver *(top)* and serum *(bottom)* levels of triglycerides and free fatty acids of mice fed with a CSAA or CDAA for 32 and 66 weeks. Results are expressed as mean ± SEM arbitrary units of 6-7 individual mice. (C) Quantification of ceroid-laden macrophages aggregates in the liver mice fed with a CSAA or CDAA for 32 and 66 weeks. Representative images of H&E at 66 weeks were shown, where arrowhead depicts ceroid-laden macrophages. Results are expressed as mean ± SEM arbitrary units of 4 individual mice. $^{\S}p < 0.05$ from CSAA-fed WT mice; $^{\dagger}p < 0.05$ from CDAA-fed WT mice.

Figure S3

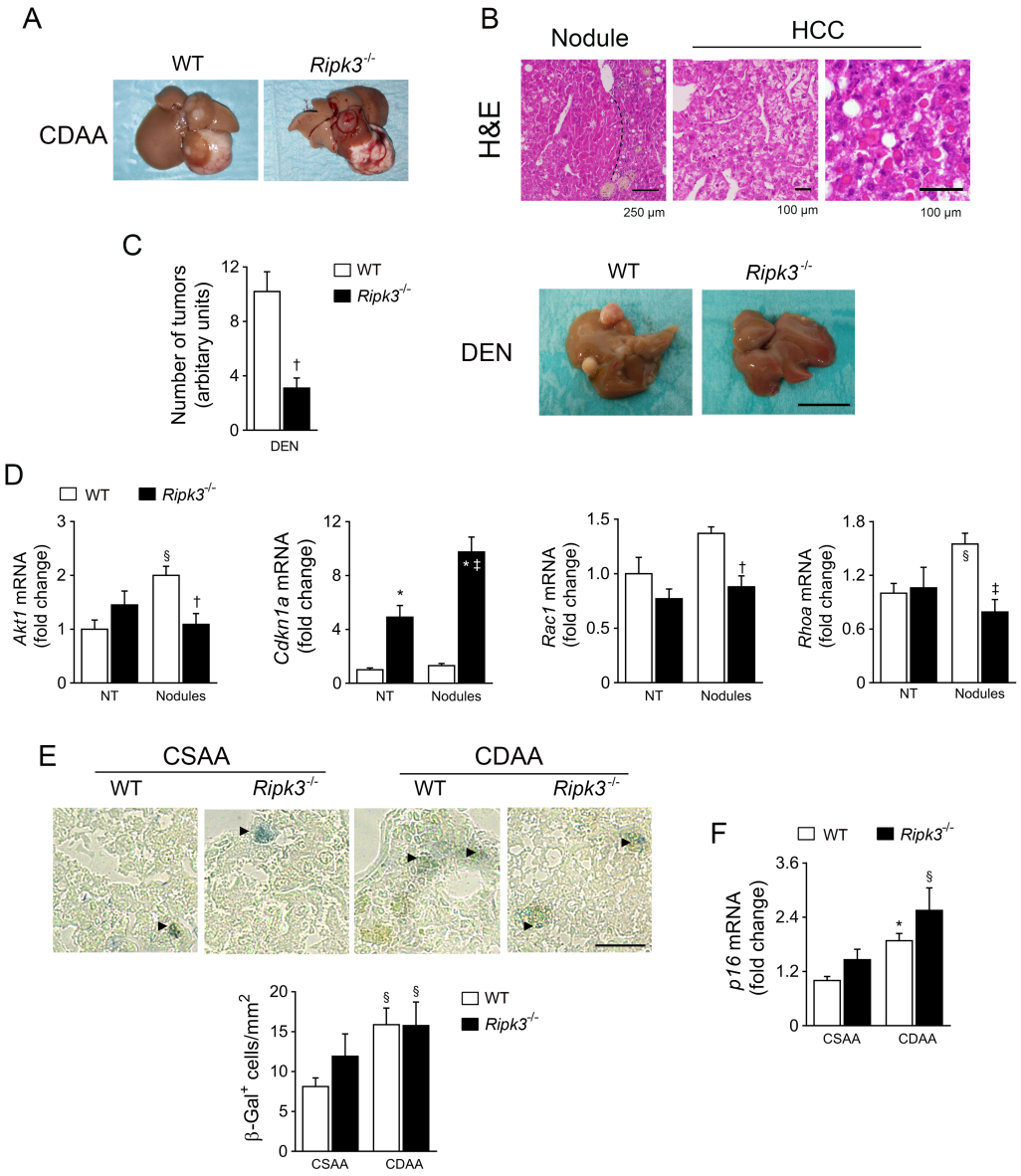

Figure S3 Histological characterization of livers from CDAA-fed mice for 66 weeks and gene array validation. C57BL/6 WT or *Ripk3*$^{-/-}$ mice were fed a CDAA or an isocaloric control CSAA diet for 66 weeks. (A) Representative macroscopic images of livers that developed HCC. (B) Representative images of H&E stained preneoplastic nodules and HCC. Nodule borders are indicated by a dashed line. (C) Number of tumours induced by DEN in WT or C57BL/6 WT or *Ripk3*$^{-/-}$ mice at the age of 42 weeks. Representative macroscopic images of livers are shown. The scale bar represents 1 cm. (D) qRT-PCR analysis of *Akt1*, *Cdkn1a*, *Rac1* and *Rhoa* in mouse liver at 66 weeks for the validation

of RT² Profiler™ Mouse Liver Cancer PCR Array. (E) Representative staining for senescence-associated β-galactosidase. Arrowheads depict β-galactosidase-positive cells. Histogram shows the quantification of senescence-associated β-galactosidase-positive cells per tissue area. Scale bar = 30 μm. (F) qRT-PCR analysis of *p16* in mouse liver. Results are expressed as mean ± SEM fold change of 6-7 individual mice for CDAA model and 13-16 individual mice for DEN model. $^{\S}p < 0.05$ and $^{*}p < 0.01$ from NT CDAA-fed WT mice; $^{\dagger}p < 0.05$ from and $^{\ddagger}p < 0.01$ from nodules CDAA-fed WT mice.

Figure S4

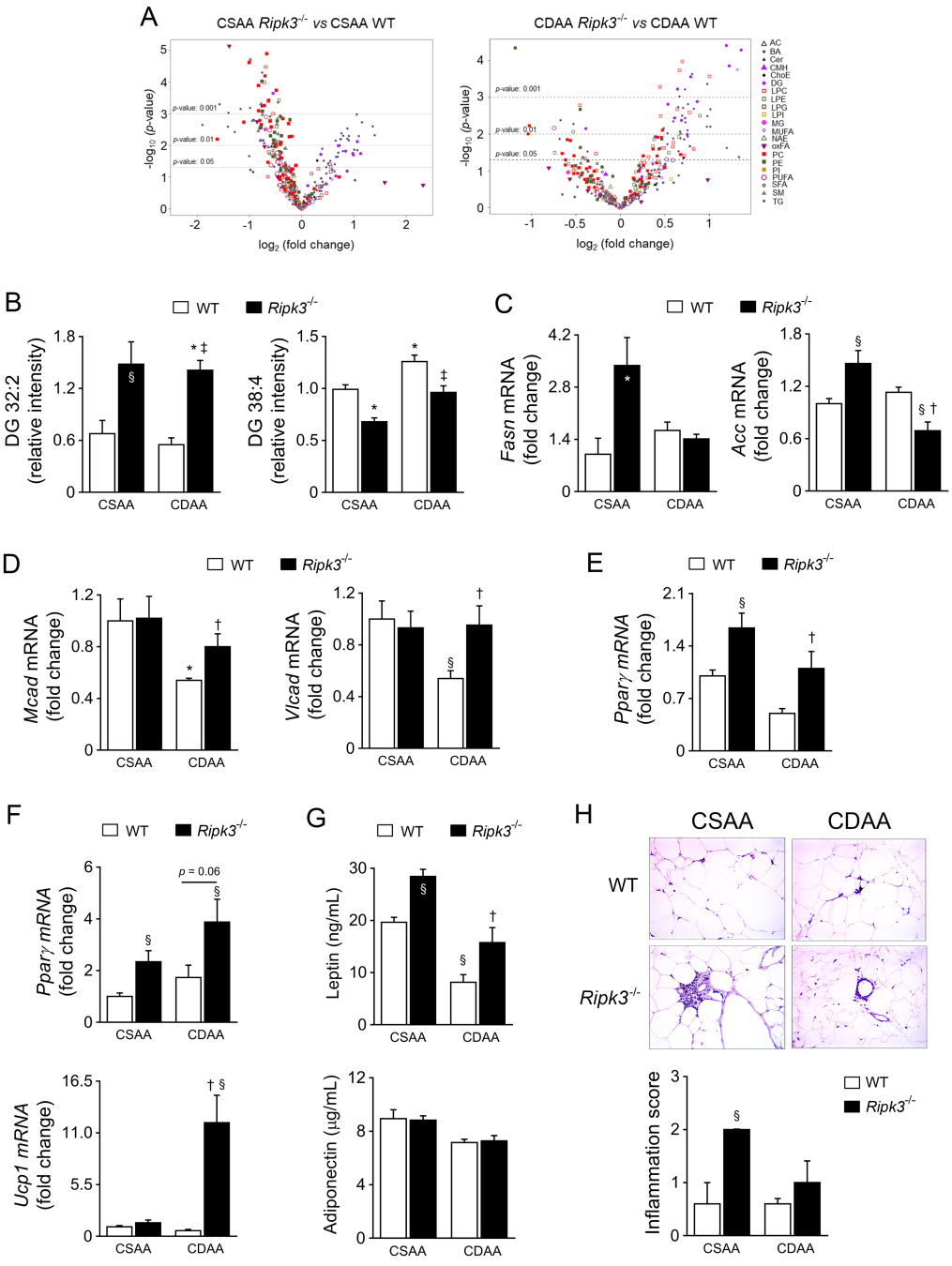

Figure S4 Impact of *Ripk3* deficiency on lipid metabolism and PPARγ expression. C57BL/6 WT or *Ripk3*$^{-/-}$ mice were fed a CDAA or an isocaloric control CSAA diet for 32 weeks. (A) Lipidomics volcano plot [-log10(*p*-value) *vs*. log2(fold-change)] for the comparison CSAA *Ripk3*$^{-/-}$ *vs* CSAA WT (*left*) and CSAA *Ripk3*$^{-/-}$ *vs* CSAA WT (*right*). AC, acyl carnitines; BA, bile acids; Cer, ceramides; ChoE, cholesteryl esters; CMH,

monohexosylceramides (cerebrosides); DG, diglycerides; LPC, lysophosphatidylcholine; LPE, lysophosphatidylethanolamine; LPI, lysophosphatidylinositols; MG, monoglycerides; MUFA, monounsaturated fatty acids; NAE, N-acyl ethanolamines; oxFA, oxidised fatty acids; PC, phosphatidylcholines; PE, phosphatidylethanolamines; PG, phosphatidylglycerols; PI, phosphatidylinositols; PUFA, polyunsaturated fatty acids; SFA, saturated fatty acids; SM, Sphingomyelins; TG. triglycerides. (B) Relative intensity of two selected DG, representing DG with shorter acyl chains and low unsaturation levels (DG 32:2) and longer acyl chains and higher number of double bonds (DG 38:4). (C) qRT-PCR analysis of *Fasn* and *Acc* in mouse liver. (D) qRT-PCR analysis *of Mcad* and *Vlcad* in mouse liver. (E) qRT-PCR analysis of *Pparγ* in mouse liver. (F) qRT-PCR analysis *Pparγ* and *Ucp1* in mouse epididymal white adipose tissue. (G) Serum leptin and adiponectin levels from mouse. Results are expressed as mean ± SEM arbitrary units or fold change of 6-7 individual mice. (H) Representative images of H&E stained white adipose tissue cryosections *(top)*. Histogram shows the inflammation score un blinded adipose tissue samples. Results are expressed as mean ± SEM arbitrary units or fold change of 4 individual mice. $^{\S}p < 0.05$ and $^{*}p < 0.01$ from NT CDAA-fed WT mice; $^{\dagger}p < 0.05$ from and $^{\ddagger}p < 0.01$ from nodules CDAA-fed WT mice.

Figure S5

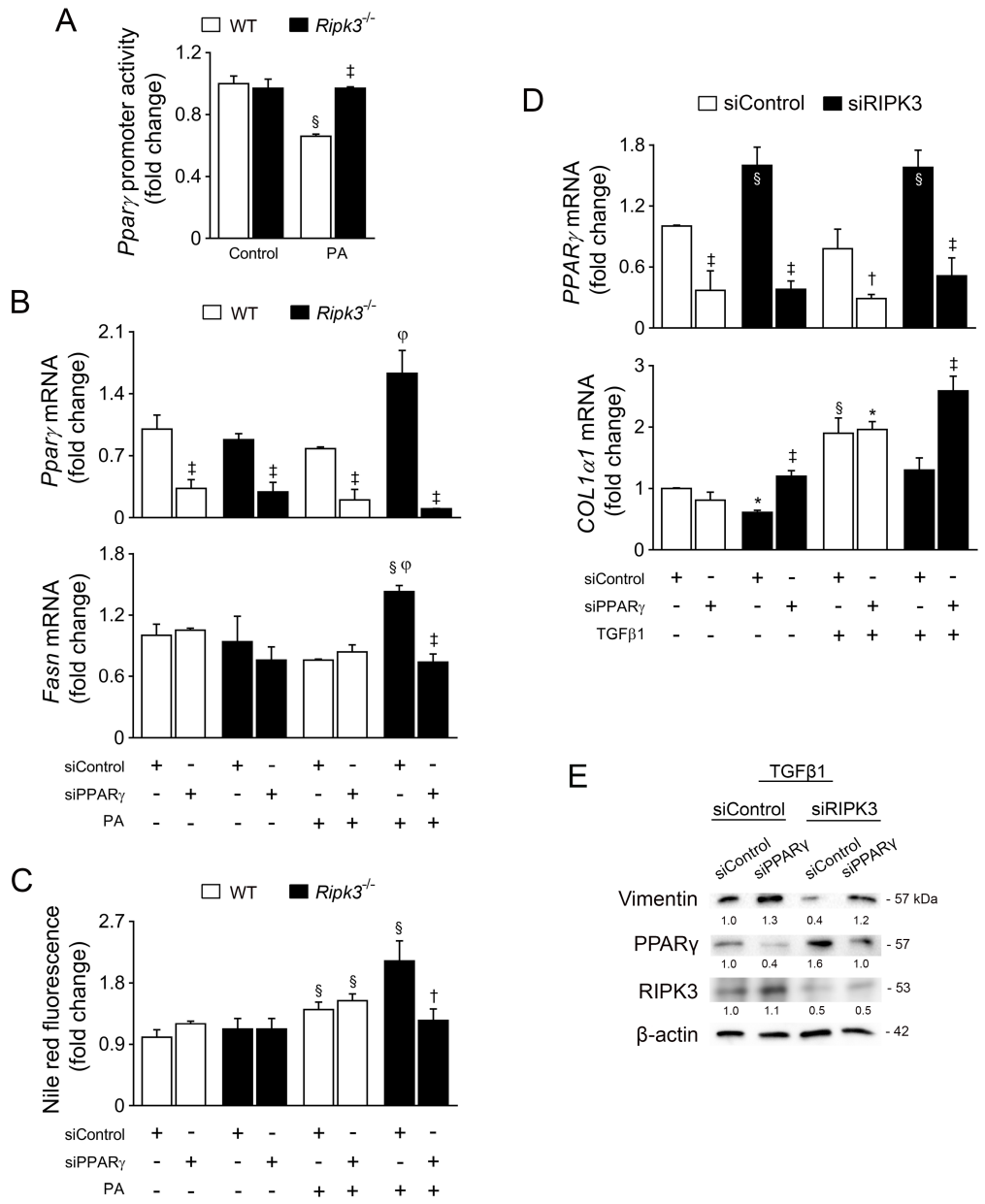

Figure S5 *In vitro* mechanistic studies to dissect the role of PPARγ in RIPK3 deficiency -associated phenotype. **A.** Primary mouse hepatocytes isolated from Wt and *Ripk3*$^{-/-}$ mice were transfected with a *Pparγ*-promoter Gaussian luciferase reporter construct for 16h, and then treated with PA or vehicle control for 24 hours. Secreted alkaline phosphatase signal was used as an internal standard control. **B.** Primary mouse hepatocytes isolated from Wt and *Ripk3*$^{-/-}$ mice were transfected with a siRNA targeting *Pparγ* (siPPARγ) or a scrambled control (siControl) for 16h. Then, cells were loaded with

PA or vehicle control for 24 hours and harvested RNA extraction or Nile red fluorometric quantification. qRT-PCR analysis *of Pparγ (top)* and *Fasn (bottom)*. **C.** Fluorometric measurement of Nile red staining normalized for total protein content. **D.** LX-2 cells were co-transfected with siRNA against human PPARγ and RIPK3 or siControl in 4 different combinations: 1) siControl; 2) siControl + siPPARγ; 3) siRIPK3 + siControl; 4) siRIPK3 + siPPARγ) for 24 hours. Cells were then treated with TGFβ1 for 24 hours and harvested for total protein and RNA isolation. qRT-PCR analysis *of PPARγ (top)* and *COL1α1 (bottom)* **E.** Representative immunoblots and densitometry of Vimentin, PPARγ, and RIPK3, PTEN. β-actin was used as a loading control. $^{\S}p < 0.05$ and $^{*}p < 0.01$ from control; $^{\dagger}p < 0.05$ from and $^{\ddagger}p < 0.01$ from respective control. $^{\varphi}p < 0.01$ from control WT hepatocytes treated with PA.